Sigma J Eng & Nat Sci 37 (2), 2019, 341-360

Sigma Journal of Engineering and Natural Sciences
Sigma Mühendislik ve Fen Bilimleri Dergisi

Research Article

ANALYTICAL STUDY OF A TWO-PHASE REVOLVING SYSTEM OF NANOFLUID FLOW IN THE PRESENCE OF A MAGNETIC FIELD TO IMPROVE HEAT TRANSFER

Mosayeb GHOLINIA[1], Hossein JAVADI*[2], Ali GATABI[3], Amirhossein KHODABAKHSHI[4], Davood Domiri GANJI[5]

[1]*Mazandaran University of Science and Technology, Faculty of Mechanical Engineering, Babol-IRAN;*
ORCID: 0000-0001-8291-8824
[2]*Mazandaran University of Science and Technology, Faculty of Mechanical Engineering,Babol-IRAN;*
ORCID: 0000-0002-2059-7145
[3]*Mazandaran University of Science and Technology, Faculty of Mechanical Engineering, Babol-IRAN;*
ORCID:0000-0002-3454-452X
[4]*Mazandaran University of Science and Technology, Faculty of Mechanical Engineering, Babol-IRAN;*
ORCID:0000-0003-2699-3699
[5]*Babol Noshirvani University of Technology, Faculty of Mechanical Engineering, Babol-IRAN;*
ORCID: 0000-0002-4293-5993

Received: 19.06.2018 Revised: 14.11.2018 Accepted: 23.12.2018

ABSTRACT

In this research, heat transfer of nanofluid flow in a two-phase revolving system considering the magnetic field is investigated. The fundamental partial differential equations of momentum, mass, and energy reduced to the nonlinear ordinary differential equations which are solved using Akbari-Ganji's Method (AGM). The introduced method solves problems based on the Trial Function. The comparison between the numerical (Runge-Kutta Fourth-Order Method) and analytical results indicates great agreement in solving the nonlinear differential equations. Also, the impact of Schmidt (Sc) number and parameters such as Brownian (Nb) parameter, Magnetic parameter (M), Melting parameter (δ), Viscosity parameter (R), Rotating parameter (Kr), and Thermophoretic (Nt) parameter on the profiles of velocity (g(η), f'(η), f(η)), temperature (θ), concentration (ϕ), Nusselt number (Nu), and surface friction coefficient (C_f) are studied. Conclusions show that by the increase in Viscosity parameter, the temperature profile increases in the range of [0, 1], but with the increase in Melting parameter, temperature profile decreases. In addition, by increasing Rotating parameter or decreasing Brownian parameter, the surface friction coefficient profile increases from top to bottom plate. Furthermore, the results show that nanofluid heat transfer rate in a two-phase revolving system can be improved by controlling the magnetic field.

Keywords: Stretching sheet, Akbari-Ganji's Method (AGM), melting heat transfer, magnetic field, rotating system, nanofluid flow.

* Corresponding Author: e-mail: h.javadi994@ustmb.ac.ir, tel: +98 (937) 818 5556

1. INTRODUCTION

Magneto hydrodynamics (MHD) also magneto-fluid dynamics or hydro magnetics is the study of magnetic properties of electrically conducting fluids. Examples of such magneto fluids include plasmas, liquid metals, salt water, and electrolytes. The fundamental concept of MHD is that magnetic field can induce flows in a moving conductive fluid, which leads to polarizing the fluid and changing the magnetic field. The set of equations that describe MHD are a combination of the Navier–Stokes equations of fluid dynamics and Maxwell's equations of electro-magnetism. These differential equations must be solved simultaneously, either analytically or numerically. Melting is a thermal process that results in the phase transition of a substance from solid to liquid. The internal energy of a substance which is increased by having high heat or pressure results in a rise of temperature to the melting point, at which the ionic or molecular structures in a solid break down and the solid liquefies. Molten substances generally have reduced viscosity with elevated temperature; an exception to this maxim is the element sulfur, whose viscosity increases to a point due to polymerization and then decreases with higher temperatures in its molten state. Nanofluids are primarily used for their enhanced thermal properties as coolants in heat transfer equipment such as heat exchangers, electronic cooling system (such as flat plate) and radiators. However, they are also useful for their controlled optical properties. Using Nanofluids in the solar collectors is another application of them which are useful because of their tunable optical properties.

Qayyum et al. [1] analyzed simultaneously the results of melting heat transfer and inclined magnetic field flow of hyperbolic tangent fluid across a nonlinear stretching surface with homogeneous-heterogeneous reactions. The outcomes indicated that improvement in wall concentration is achieved by the higher strength of homogeneous and heterogeneous reactions. Besides, a rise in space and temperature dependent non-uniform heat source/sink variables show an increase in temperature. In the other research, based on what has been claimed by Ibrahim [2], the melting heat transfer in the magneto hydrodynamic stagnation point flow of a Nanofluid passing a stretching sheet was examined; the results showed that a rise in melting parameter led to increasing in the velocity, thermal and concentration boundary layer thickness. Additionally, an increase in the values of melting parameter increased the skin friction coefficient, local heat and mass transfer rate. The impacts of thermophoresis diffusion and thermally developed Brownian motion on non-Newtonian Nanofluid through an inclined stretching surface with the effect of chemical reaction, and thermal radiation were studied by Gupta et al. [3]. They concluded that the velocity of fluid was reduced with an increase in Magnetic parameter and was increased with an increase in buoyancy ratio. Moreover, their experimental and theoretical studies illustrated that temperature was increased with an increase in Brownian motion parameter, buoyancy ratio, and thermophoresis parameter, but was decreased with increasing in the values of Lewis number and Prandtl number. Also, they believed that nanoparticles concentration was decreased with the increases of Brownian motion parameter, while it was increased by increasing in thermophoresis parameter. Some studies have been conducted for evaluating the effects of Lorentz forces on heat transferring of Nanofluid flow [4-9]. Simulation of convective heat transfer of MHD Nanofluid flow in a box included hot barrier was done by Sheikholeslami et al. [7]. Their results showed that higher Darcy number leads to an increase in convective heat transfer. Also, conduction mode can be stronger in comparison with convection mode in the presence of Lorentz forces. Influence of Lorentz forces on forced-convection Nanofluid flow over a stretched surface was investigated by Sheikholeslami et al. [10]. Gireesha et al. [11] performed a numerical analyze on a steady two-dimensional hydro magnetic stagnation point flow of an electrically conducting Nanofluid passing a stretching surface by considering magnetic field, melting effect and heat generation/absorption. Their results have a similar physical agreement with the work of Hsiao [12] who has studied the heat and mass mixed convection for magneto hydrodynamic viscoelastic fluid past a stretching sheet with Ohmic dissipation. They found that the induced magnetic field and temperature distributions magnified with the strengthening of the hydro magnetic field. They also found that

heat transfer capability of the base fluid improves when there are suspended nanoparticles in the fluid. Zhang et al. [13] built th e power-law fluid governing equations with changeable thermal conductivity. They also investigated on the effects of variable magnetic field and velocity slip on the flow of incompressible pseudo-plastic ethylene vinyl acetate copolymer (EVA) Nanofluid in a finite film over a stretching sheet. Their studies indicated that as the slip parameter increases the temperature, it leads to thinner film thickness. The influence of Prandtl number on the thickness of thin film is almost negligible. Transportation of MHD nanofluid free convection in a porous semi annulus using numerical approach was studied by Sheikholeslami and Ganji [14]. By using the Cattaneo–Christov heat flux model and considering thermal radiation effect, heat transfer and unsteady squeezing flow of Nanofluid between a penetrable disk and a stretchable one were investigated by Dogonchi et al. [15]. Based on their results, there is an inverse relationship between stretching parameter and the Nusselt number, although both of the suction and injection parameters and the magnitude of the shrinking parameter have a direct relationship with the Nusselt number. Furthermore, there are some investigations on the influence of thermal radiation effect on the flow and heat transfer of MHD Nanofluid between plates [15-22]. By considering thermal radiation when MHD Go-water Nanofluid flows between two parallel plates, heat transfer between them was studied by Dogonchi et al. [19]. According to their results, it can be seen that there is an inverse relationship between radiation parameter with temperature profile and the Nusselt number, as well as a direct relationship between solid volume fraction with temperature profile and the Nusselt number. In other research, Bai et al. [23] investigated mass and heat transfer at Stagnation-point of MHD Maxwell Nanofluids over a stretching plate in existence of thermophoresis. Their studies demonstrated that a drop in the fluid flow was followed by an increasing in the Maxwell and magnetic parameters. Khan et al. [24] done a numerical investigation on the influence of nonlinear radiative heat flux mechanisms and melting heat transfer for an incompressible generalized Burgers fluid. According to their findings, an increase in the melting and radiation parameters resulted in a decrease in the temperature contour, though, the associated boundary layer thickness was improved. Sheikholeslami [27] used Lattice Boltzmann Method in order to simulate Nanofluid flow in a 3D porous cavity and in the presence of magnetic field. The results indicated that the Nusselt number will be decreased by increasing Lorentz forces. Also, it was concluded that Darcy number and Reynolds number have a direct relationship with gradient temperature. There are lots of studies that investigated using Nanofluid in porous media [4-7,9,19,25-31]. Mehrez et al. [32] studied an outer-oriented magnetic field of Cu–water Nanofluid flow in an open cavity heated from below numerically to investigate the heat transfer and entropy generation. Their findings showed that the flow behavior, the heat transfer and entropy generation and their changes rates depend on the concentration and orientation of the magnetic field. For all the studied cases, the average Nusselt number and the average entropy generation increased, as well as, the Bejan number decreased by increasing in the volume fraction of solid nanoparticles. Another study was carried out by Rana et al. [33]. They explored the impact of electrically conducting alumina-water Nanofluid flow which was caused by horizontal shrinking cylinder under the influence of velocity and thermal slip. They used the Buongiorno's non-homogenous model which accounted for the Nano layer based effective thermal conductivity and Nielsen's effective viscosity model. Their work showed that friction at the surface increased with the improvement of the magnetic field. However, friction at the surface was decreased by velocity slip parameter and curvature parameter. Mahanthesh et al. [34] performed an analytical research to explore the effects of heat and mass transfer on unsteady magneto hydrodynamic free convection flow of chemically reacting Nanofluid passing a moving and stationary vertical plate. Based on the results, drag force at the plate was reduced as a result of increasing magnetic field strength. On the other hand, they accounted the opposite trend as nanoparticle volume fraction changed. In another study [35] they did a theoretical investigation on nonlinear radiative heat transfer in MHD three-dimensional flow including water-based Nanofluid over a non-linearly stretching sheet with convective boundary condition. Their investigation showed that changing

the nanoparticle volume fraction controlled the attributes of the fluid. Moreover, the types of nanoparticles have influence on flow characteristics. They also studied [36] the problem of unsteady three-dimensional MHD flow of a Nano Eyring-Powell fluid through a convectively heated stretching sheet with the presence of thermal radiation, viscous dissipation, and Joule heating. The conclusions showed that the velocity field was more significant for Nano Eyring-Powell fluid than that of a regular fluid. Additionally, the influence of applied magnetic field reduced the velocity profile whereas opposite behavior was found for Eyring-Powell fluid parameter. Using DTM-Padé approach to squeezing Cu–water Nanofluid flow analysis between parallel plates was studied by Domairry and Hatami [37]. In their work, Pade approximation and differential transformation method (DTM) are implemented, and with the use of the Maxwell–Garnetts model, effective thermal conductivity is calculated. They found that Nusselt number increase with the rise of nanoparticle volume fraction. Krishnamurthy et al. [38] made a numerical investigation on the impact of chemical reaction on melting heat transfer and MHD boundary layer of Williamson Nanofluid in a porous medium. The outcome illustrated velocity and the boundary layer thickness increased and temperature distribution decreased with an increase in melting parameter. Another numerical study carried out by Bao et al. [39]. They used alternating magnetic fields to improve the convective heat transfer in liquid oxygen. They observed that the vortex formation and shedding caused fluctuation of the thermal boundary layer and mixing of cold and hot fluids, which advanced the heat transfer notably. Hayat et al. [40] presented the influences of Cu–water MHD Nanofluid flow with viscous dissipation and Joule heating over a stretching sheet with the consideration of melting heat transfer and effects of viscous dissipation in their work. The results demonstrated that velocity profile was decreased by an increase in the nanoparticle volume fraction, and increasing in melting parameter enhanced the velocity and reduced the temperature. Also, temperature profile increased when the volume fraction of copper nanoparticles increased. Sheikholeslami and Rokni [41] used the Buongiorno model to study the impression of melting heat transfer on Nanofluid flow in the presence of a magnetic field. Their outcomes confirmed that the velocity and concentration were increased by increasing the melting parameter, however, the temperature decreased. In another research [42] they employed two-phase model and studied the impact of melting parameter on MHD Nanofluid flow. The outcomes demonstrated that Nusselt number increased with a rise of Lorentz forces, but it decreased with augmented Reynolds number and Eckert number. [43] studied the influence of melting on Nanofluid flow and heat transfer inside a cavity in the presence of magnetic field. It has been found that temperature gradient developed with an increment of melting parameter and Rayleigh number.

At the heart of all different engineering sciences, all phenomena show themselves in a mathematical relationship modeled in the form of differential equations. Most of these mathematical relationships are in nonlinear form. Among the nonlinear relationships used in fluid mechanics there are Newtonian and non-Newtonian fluids problems for which we need an analytical method that can minimize the solution error in comparison with the numerical solution. There are lots of articles that had studied different problems by using analytical methods [44-48]. In general, analytical methods can be divided into two types based on their solution stages:

- Methods that solve problems based on Iterate-base
- Methods that solve problems based on Trial Function-base

In the Iterate-based methods such as HAM, VIM etc., the important factors that affect the solution is the number of repetitions. In this way, the previous stage must be resolved in order to achieve a solution for each stage. It is worth noting that if the previous stage cannot be solved, the software will not be able to solve the next stages, which will lead to disruption in solving the problem. But in the methods such as GM and LSM the important factor is the Trial Function. In these methods, the problem solving begins by selecting an appropriate test function which is assumed on the basis of the initial and boundary conditions. The important point in the test

function is the constant factors which are generally obtained by solving polynomial equations. The results obtained from the aforementioned points show that the methods which solve the problems based on the Trial Function do not have the problems of the repetition solution method. It is worth mentioning that Akbari-Ganji's Method (AGM) is a modern method based on the Trial Function which is useful for studying the nonlinear issues. Notable feature of this method is as follow: Boundary conditions are needed in accordance with the order of differential equations in the solution procedure, but when the number of boundary conditions is less than the order of the differential equations, this approach can create additional new boundary conditions in regard to the derivatives and its own differential equation. AGM is a new powerful approach for solving various nonlinear differential equations. Some of the advantages of this method are as follows: AGM is a suitable computational process for solving diverse and more difficult nonlinear differential equations in many fields. It is very simple, straightforward, precise and has short stages to obtain the analytical answer. Moreover, in this specified nonlinear differential equation, AGM has an acceptable precision in comparison with numerical method, as it has been shown in the results. In fact, the most important advantage of AGM is its high computational speed in solving nonlinear ordinary differential equations.

In this paper, we have applied a new analytical method of Akbari–Ganji's method (AGM) to find the solution of a nonlinear problem using Nanofluid flow in the presence of magnetic field in a two-phase revolving system to improve heat transfer. Also, the impact of Schmidt (Sc) number, Brownian (Nb) parameter, Magnetic parameter (M), Melting parameter (δ), Viscosity parameter (R), Rotating parameter (Kr) and Thermophoretic (Nt) parameter on the profiles of velocity (g(η), f'(η), f(η)), temperature profile (θ), concentration profile (ϕ), Nusselt number profile and surface friction coefficient (C_f) profile are investigated. Moreover, the comparison between the results of AGM and some numerical and semi-analytical methods illustrates an excellent agreement in solving this nonlinear issue.

2. PROBLEM DESCRIPTION

The steady Nanofluid flow within two parallel plates when the fluid and the plates revolve together around the y-axis is considered in the form of normal to the plates with an angular velocity. Fig. 1 shows a Cartesian coordinate system that is granted as followed: the y-axis is vertical to the plate, the x-axis is along it, and the z-axis is normal to the x-y plane. A uniform magnetic flux with density B_0 is acting along y-axis around which the system is turning. The plates are positioned at y=h and y= 0. The below plate is being pulled by two contrary and equal forces so that the location of the point (0,0,0) remains constant. The governing equations in a rotating frame are given [49]:

$$\frac{\partial u}{\partial x}+\frac{\partial v}{\partial y}+\frac{\partial w}{\partial z}=0 \tag{1}$$

$$\rho_f\left\{u\frac{\partial u}{\partial x}+v\frac{\partial u}{\partial y}+2\Omega w\right\}=-\frac{\partial p^*}{\partial x}+\mu\left\{\frac{\partial^2 u}{\partial x^2}+\frac{\partial^2 u}{\partial y^2}\right\}-\sigma B_0^2 u, \tag{2}$$

$$\rho_f\left\{v\frac{\partial v}{\partial y}\right\}=-\frac{\partial p^*}{\partial y}+\mu\left\{\frac{\partial^2 v}{\partial x^2}+\frac{\partial^2 v}{\partial y^2}\right\}, \tag{3}$$

$$\rho_f\left\{u\frac{\partial w}{\partial x}+v\frac{\partial w}{\partial y}-2\Omega w\right\}=\mu\left\{\frac{\partial^2 w}{\partial x^2}+\frac{\partial^2 w}{\partial y^2}\right\}-\sigma B_0^2 w, \tag{4}$$

$$u\frac{\partial T}{\partial x}+v\frac{\partial T}{\partial y}+w\frac{\partial T}{\partial z}=\alpha\left\{\frac{\partial^2 T}{\partial x^2}+\frac{\partial^2 T}{\partial y^2}+\frac{\partial^2 T}{\partial z^2}\right\}++\frac{(\rho c_p)_p}{(\rho c_p)_f}$$

$$\left[D_B\left\{\frac{\partial C}{\partial x}.\frac{\partial T}{\partial x}+\frac{\partial C}{\partial y}.\frac{\partial T}{\partial y}+\frac{\partial C}{\partial z}.\frac{\partial T}{\partial z}\right\}+(\frac{D_T}{T_c})\left\{(\frac{\partial T}{\partial x})^2+\left(\frac{\partial T}{\partial y}\right)^2+\left(\frac{\partial T}{\partial z}\right)^2\right\}\right], \quad (5)$$

$$u\frac{\partial C}{\partial x}+v\frac{\partial C}{\partial y}+w\frac{\partial C}{\partial z}=D_B\left\{\frac{\partial^2 C}{\partial x^2}+\frac{\partial^2 C}{\partial y^2}+\frac{\partial^2 C}{\partial z^2}\right\}+(\frac{D_T}{T_0})\left\{\frac{\partial^2 T}{\partial x^2}+\frac{\partial^2 T}{\partial y^2}+\frac{\partial^2 T}{\partial z^2}\right\}, \quad (6)$$

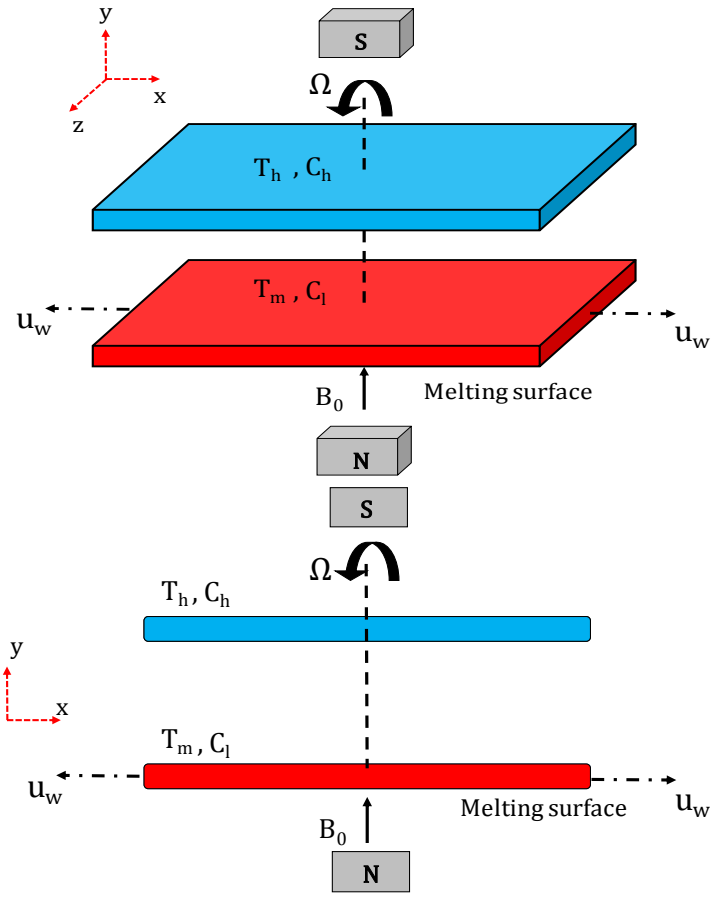

Figure 1. Schematic representation of the considered issue.

Where z, v and u are the velocities in the z, y and x directions, respectively, and C is the concentration, D_B is the diffusion coefficient of the diffusing species, μ is the dynamic viscosity, k is the thermal conductivity, ρ_f is the base fluid density, T is the temperature, C_P is the specific heat of Nanofluid and p* is the modified fluid pressure.

The following non-dimensional variables are presented:

$$\eta = \frac{y}{h},\ u = axf'(\eta), v = -ahf(\eta),\ w = axg(\eta),\ \ \theta(\eta) = \frac{T - T_m}{T_m - T_0},\ \ \phi(\eta) = \frac{C - C_0}{C_h - C_0} \quad (7)$$

A prime expresses differentiation concerning η. The associated boundary conditions are:

$$u = ax, k(\frac{\partial T}{\partial y})_{y=0} = \rho_f (L + c_s(T_m - T_0))v, \quad w = 0, \quad T = T_m, \quad C = C_0 \Rightarrow y = 0$$
$$u = 0, \quad v = 0, \quad w = 0, \quad T = T_h, \quad C = C_h \Rightarrow y = +h \quad (8)$$

C_s is the heat capacity of the solid surface and L is the non-uniform latent heat of the fluid. The lack of $\frac{\partial P^*}{\partial z}$ in Eq. (4) indicates that there is a cross-flow along the z-axis.

The boundary condition of (7) shows that the heat conducted to the melting face is alike to the heat of melting plus the heat demanded to increase the solid temperature of T_0 to its melting temperature of T_m [50].

By substituting (8) in Eqs. (1)– (4), we obtain:

$$-\frac{1}{\rho h}\frac{\partial p^*}{\partial \eta} = a^2 x\left[f' - ff'' - \frac{f'''}{R} + \frac{M}{R} + \frac{2Kr}{R}g\right], \quad (9)$$

$$-\frac{1}{\rho h}\frac{\partial p^*}{\partial \eta} = a^2 h\left[ff' + \frac{1}{R}f''\right], \quad (10)$$

$$g'' - R(f'g - fg') + 2Krf' - Mg = 0 \quad (11)$$

The non-dimensional values are determined, in which Kr is the Rotating parameter, M is the Magnetic parameter and R is the Viscosity parameter.

$$R = \frac{ah^2}{\upsilon},\ M = \frac{\sigma B_0^2 h^2}{\rho\upsilon},\ \ Kr = \frac{\Omega h^2}{\upsilon} \quad (12)$$

Eq. (8) with the help of (7) can be formulated as:

$$f''' - R[f'^2 - ff''] - 2Kr^2 g - M^2 f' = A \quad (13)$$

Separation of Eq. (11) concerning η gives:

$$f^{iv} - R[f'f'' - ff''] - 2Krg' - Mf'' = 0 \quad (14)$$

Moreover, Eqs. (5) and (6) convert to:

$$\theta'' + Pr Rf\theta' + Nb\phi'\theta' + Nt\theta'^2 = 0, \quad (15)$$

$$\phi'' + R.Scf\phi' + \frac{Nt}{Nb}\theta'' = 0, \quad (16)$$

Thus, the governing equations for this problem in non-dimensional appearance are given by:

$$f^{iv} - R[f'f'' - ff''] - 2Krg' - Mf'' = 0 \quad (17)$$

$$g'' - R[f'g - fg'] + 2Krf' - Mg = 0 \quad (18)$$

Boundary conditions are:

$$f(0) = -\frac{\delta}{Pr}\theta'(0),\ \ f' = 1,\ g = 0,\ \theta = 0,\ \ \phi = 0 \Rightarrow \eta = 0$$
$$f = 0,\ \ f' = 0,\ \ g = 0,\ \ \theta = 1,\ \phi = 1 \Rightarrow \eta = 1 \tag{19}$$

Here δ is Melting parameter, Nt is Thermophoretic parameter, Sc is the Schmidt number, Nb is the Brownian motion parameter and Pr presents the Prandtl number which are described as:

$$Pr = \frac{\mu}{\rho_f a},\quad Sc = \frac{\mu}{\rho_f D},\quad Nb = (\rho c)_p D_B (C_h)/((\rho c)_f a),$$
$$Nt = (\rho c)_p D_T (T_H)/((\rho c)_f a T_c),\quad \delta = \frac{(\rho c)_p}{\rho_f}\frac{(T_h - T_m)}{1 + c_s (T_m - T_0)} \tag{20}$$

Skin friction coefficient (C_f) and Nusselt number (Nu) along the stretching wall are defined as:

$$\tilde{C}_f = (Rx/h)C_f = f''(0), Nu = -\theta'(0) \tag{21}$$

It should be noted that δ is a combination of the Stefan numbers $C_s\ (T_m - T_0)/L$ and $C_P\ (T_\infty - T_m)/L$ for the solid and liquid states, respectively.

3. DESCRIPTION OF AKBARI-GANJI'S METHOD (AGM)

Primary conditions and boundary conditions are needed differential equations conforming to the considered problem. Therefore, we can solve every differential equation with any degree. In order to understand the given method in this research, two differential equations ruling on engineering operations will be solved in this new method. The nonlinear differential equation of p which is a function of u (which is a function of x), and their derivatives are considered as follows:

$$p_k : f(u, u', u'', \ldots u^m) = 0\ ; u = u(x), \tag{22}$$

Boundary conditions:

$$\begin{cases} u(0) = u_0, u'(0) = u_1, \ldots u^{(m-1)}(0) = u_{m-1} \\ u(L) = u_{L0}, u'(L) = u_{L1}, \ldots u^{(m-1)}(L) = u_{Lm-1} \end{cases} \tag{23}$$

To solve the first differential equation, with respect to the boundary conditions in $x = L$ in Eq. (23), the series of letters in the $n\ th$ order by constant coefficients, which is the reply of the first differential equation, is considered as follows:

$$u(x) = \lim_{n\to\infty} \sum_{i=0}^{n} a_i x^i = \lim_{n\to\infty} (a_0 + a_1 x^1 + a_2 x^2 + \ldots a_n x^n), \tag{24}$$

The boundary conditions are applied to the function as follows:

a) The application of the boundary conditions for the reply of differential Eq. (24) is in the form of:
If $x = 0$

$$\begin{cases} u(0) = a_0 = u_0 \\ u'(0) = a_1 = u_1 \\ u''(0) = a_2 = u_2 \\ \vdots \quad \vdots \quad \vdots \end{cases} \tag{25}$$

and when $x = L$

$$\begin{cases} u(0) = a_0 + a_1 L + a_2 L^2 + ... + a_n L^n = u_{L_0} \\ u'(0) = a_1 + 2a_2 L + 3a_3 L^2 + ... + n a_n L^{n-1} = u_{L_1} \\ u''(0) = 2a_2 + 6a_3 L + 12 a_4 L^2 + ... + n(n-1) a_n L^{n-2} = u_{L_{m-1}} \\ \vdots \quad \vdots \quad \vdots \quad \vdots \quad \vdots \quad \vdots \end{cases} \tag{26}$$

After substituting Eq. (26) into Eq. (22), the application of the boundary conditions on differential Eq. (22) is done according to the following procedure:

$$\begin{aligned} & p_0 : f(u(0), u'(0), u''(0), ... u^{(m)}(0)) \\ & p_1 : f(u(L), u'(L), u''(L), ... u^{(m)}(L)) \\ & \vdots \quad \vdots \quad \vdots \quad \vdots \quad \vdots \end{aligned} \tag{27}$$

With attention to the selection of n; ($n < m$) sentences from Eq. (24) and in order to make a set of equations which is consisted of $(n + 1)$ equations and $(n + 1)$ unknowns, we confront with a number of additional unknowns which are indeed the same coefficients of Eq. (24). So, to solve this issue, we should derive m from Eq. (22) according to the additional unknowns in the aforementioned set differential equations and then this is the time to apply the boundary conditions of Eq. (23) on them.

$$\begin{aligned} & p_k' : f'(u', u'', u''', ... u^{(m+1)}) \\ & p_k'' : f''(u'', u''', u^{IV}, ... u^{(m+2)}) \\ & \vdots \quad \vdots \quad \vdots \quad \vdots \end{aligned} \tag{28}$$

b) Usage of the boundary conditions on the derivatives of the differential equation P_k in Eq. (28) is done in the form of:

$$p_k' : \begin{cases} f'(u'(0), u''(0), u'''(0), ..., u^{(m+1)}(0)) \\ \\ f'(u'(L), u''(L), u'''(L), ..., u^{(m+1)}(L)) \end{cases} \tag{29}$$

$$p_k'' : \begin{cases} f''(u''(0), u'''(0), ..., u^{(m+2)}(0)) \\ \\ f''(u''(L), u'''(L), ..., u^{(m+2)}(L)) \end{cases} \tag{30}$$

The $(n+1)$ equations can be created from Eq. (25) to Eq. (30) so that $(n+1)$ unknown coefficients of Eq. (24) for instance, $a_0 + a_1 + a_2 + a_3 + \cdots a_n$ can be calculated. The reply of the nonlinear differential Eq. (22) will be achieved by defining coefficients of Eq. (24).

4. APPLICATION OF THE AKBARI-GANJI'S METHOD (AGM)

By considering the fundamental idea of the method, we rewrite the Eqs. (15-18) in the following order:

$$\begin{aligned} &F(\eta) = f^{IV} - R(f'.f'' - f.f''') - 2Kr.g' - M.f'' = 0, \\ &G(\eta) = g'' - R(f'.g - f.g') + 2Kr.f' - M.g = 0, \\ &\Theta(\eta) = \theta'' + Pr.R.f.\theta' + Nb.\phi'.\theta' + Nt.\theta'^2 = 0 \\ &\Phi(\eta) = \phi'' + R.Sc.f.\phi' + (Nt/Nb).\theta'' = 0 \end{aligned} \tag{31}$$

In AGM, the reply of the nonlinear differential equations is considered as a confined series of polynomials via constant coefficients, as follows:

$$f(\eta) = \sum_{k=0}^{7} a_k \eta^k = a_0 + a_1\eta + a_2\eta^2 + a_3\eta^3 + a_4\eta^4 + a_5\eta^5 + a_6\eta^6 + a_7\eta^7, \tag{32}$$

$$g(\eta) = \sum_{k=0}^{5} b_k \eta^k = b_0 + b_1\eta + b_2\eta^2 + b_3\eta^3 + b_4\eta^4 + b_5\eta^5, \tag{33}$$

$$\theta(\eta) = \sum_{k=0}^{5} c_k \eta^k = c_0 + c_1\eta + c_2\eta^2 + c_3\eta^3 + c_4\eta^4 + c_5\eta^5, \tag{34}$$

$$\phi(\eta) = \sum_{k=0}^{5} v_k \eta^k = v_0 + v_1\eta + v_2\eta^2 + v_3\eta^3 + v_4\eta^4 + v_5\eta^5, \tag{35}$$

In the proposed issue we have engaged four trial functions which contain 18 constant coefficients. The constant coefficients a_0 to a_7 , b_0 to b_7, c_0 *to* c_7 and v_0 to v_5, which can easily be calculated by using the boundary conditions and initial conditions [51].

- In AGM, the boundary conditions are used in two ways:

a) Applying the boundary conditions in Eqs. (32-35) is expressed as follows:

$$f = f(BC), \quad \theta = \theta(BC), \quad \phi = \phi(BC), \quad g = g(BC) \tag{36}$$

Therefore, the boundary conditions are used according to the Eq. (36) as follows:

$$
\begin{aligned}
&f(0) = -\delta / \Pr \theta'(0) \to a_0 = 0,\\
&f'(0) = 1 \to a_1 = 1,\\
&\theta(0) = 0 \to c_0 = 0,\\
&\phi(0) = 0 \to v_0 = 0,\\
&g(0) = 0 \to b_0 = 0,\\
&f'(1) = 0 \to a_0 + a_1 + 2a_2 + 3a_3 + 4a_4 + 5a_5 + 6a_6 + 7a_7 = 0\\
&\theta(1) = 1 \to c_0 + c_1 + c_2 + c_3 + c_4 + c_5 = 1,\\
&g(1) = 0 \to b_0 + b_1 + b_2 + b_3 + b_4 + b_5 = 0,\\
&\phi(1) = 1 \to v_0 + v_1 + v_2 + v_3 + v_4 + v_5 = 1,\\
&f(1) = 0 \to a_0 + a_1 + a_2 + a_3 + a_4 + a_5 + a_6 + a_7 = 0.
\end{aligned}
\tag{37}
$$

b) Boundary conditions which are applied in Eq. (31), are shown by *F* (η)، *G*(η) ، Θ (η), $\Phi(\eta)$, and also in their derivatives as:

$$
\begin{aligned}
&F(f(\eta)) \to F(f(BC)) = 0,\ F'(f(BC)) = 0,...\\
&\Theta(\theta(\eta)) \to \Theta(\theta(BC)) = 0,\ \ \Theta'(\theta(BC)) = 0,...\\
&G(g(\eta)) \to G(g(BC)) = 0,\ \ G'(g(BC)) = 0,...\\
&\Phi(\theta(\eta)) \to \Phi(\theta(BC)) = 0,\ \ \Phi'(\theta(BC)) = 0,...
\end{aligned}
\tag{38}
$$

We have to produce 8 additional equations from Eq. (38) in order to achieve a set of polynomials which contains of 18 equations and 18 constants. According to the above descriptions we have produced additional equations of Eq. (38) in the following order:

- 2 equations have been produced by computing acquired equations from:

$$F(f(0)) = 0, \quad F(f(1)) = 0,$$

- 2 equations have been produced by computing acquired equations from:

$$\Theta(\theta(0)) = 0, \ \ \Theta(\theta(1)) = 0,$$

- 2 equations have been produced by computing acquired equations from:

$$G(g(0)) = 0, \ \ G(g(1)) = 0,$$

- 2 equations have been produced by computing acquired equations from:

$$\Phi(\phi(0)) = 0, \ \ \Phi(\phi(1)) = 0,$$

The mentioned equations are too large to be illustrate. The differential Eqs. (15-18) are solved by implementing Akbari-Ganji's Method (R=1, Kr=1, M=1, Pr=3, Nb=Nt=0.1, Sc=1, δ=0). The constant coefficients of Eqs. (32-35) can easily be gained by using above explanations. Constant coefficients are as follows:

$$
\begin{aligned}
&a_0 = 0, a_1 = 1, a_2 = \text{-}2.05, a_3 = 1.21, a_4 = \text{-}0.33, a_5 = 0.26, a_6 = \text{-}0.11, a_7 = 0.02,\\
&b_0 = 0, b_1 = 0.15, b_2 = \text{-}1, b_3 = 1.39, b_4 = \text{-}0.5, b_5 = 0.02,\\
&c_0 = 0, c_1 = 1.31, c_2 = \text{-}0.13, c_3 = \text{-}0.64, c_4 = 0.67, c_5 = \text{-}0.2,\\
&v_0 = 0, v_1 = 0.72, v_2 = 0.13, v_3 = 0.52, v_4 = \text{-}0.55, v_5 = 0.16.
\end{aligned}
\tag{39}
$$

By replacing acquired constant coefficients from above-mentioned manner, Eqs. (32-35) could easily be yielded as follows:

$$\begin{aligned} f(\eta) &= 0.025\eta^7 - 0.118\eta^6 + 0.263\eta^5 - 0.331\eta^4 + 1.217\eta^3 - 2.057\eta^2 + 1.000\eta, \\ g(\eta) &= 0.027\eta^5 - 0.577\eta^4 + 1.397\eta^3 - 1.000\eta^2 + 0.151\eta, \\ \theta(\eta) &= -0.203\eta^5 + 0.672\eta^4 - 0.646\eta^3 - 0.1335\eta^2 + 1.311\eta, \\ \phi(\eta) &= 0.167\eta^5 - 0.551\eta^4 + 0.5258\eta^3 + 0.133\eta^2 + 0.724\eta, \end{aligned} \tag{40}$$

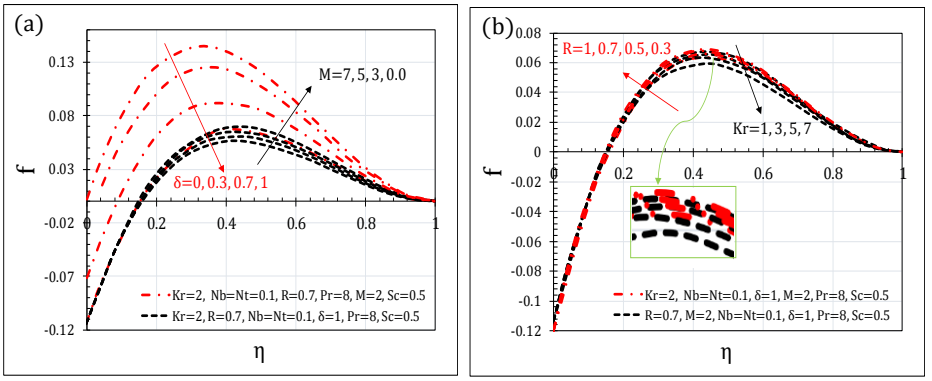

Figure 2. Influence of (a) M, δ and (b) R, Kr on velocity profiles.

Table 1. Comparison between the AGM and NUM [52] results for **f (left)** and **g (Right)**

	Nt=Nb=0.1, M=Kr= δ=1, Pr=10			Nt=Nb=0.1, M=Kr= δ=1, Pr=10		
η	NUM	AGM	Error	NUM	AGM	Error
0.0	-0.1204	-0.1211	0.0002	0.0000	0.0000	0.0000
0.2	0.0355	0.0312	-0.0043	0.0221	0.0230	0.0009
0.4	0.0688	0.0667	-0.0021	0.0120	0.0123	0.0003
0.6	0.0520	0.0538	0.0018	-0.0021	-0.0023	0.0011
0.8	0.0187	0.0199	0.0012	-0.0067	-0.0066	-0.0001
1	0.0000	0.0000	0.0000	0.0000	0.0000	0.0000

5. RESULTS AND DISCUSSIONS

In this section, we illustrate an analytical study of a two-phase revolving system of Nanofluid flow in the presence of magnetic field to improve heat transfer by implementing AGM. The AGM in this study has 18 equations and 18 constants. Although it will converge to a more accurate one by increasing the number of equations and constants, it will take more time. Thus, we obtain the following results by 18 equations for the matter of time and accuracy. In order to verify the precision of the present research, we have compared our results with the results of other published work of [52]. The comparisons are shown in Tables 1 and 2. From these tables, it can be seen that the error rates are very low. The numerical method outcomes were attained by fourth order Runge-Kutta method with Maple software package. The results illustrate that the AGM is a trustworthy approach for solving this problem. As shown in Fig. (2a), by decreasing the Magnetic parameter (M), the velocity profile f(η) has an increasing trend from the bottom plate to the top one. Moreover, with increasing in Melting parameter (δ), f(η) decreases. In Fig. (2b), the profile

of f(η) decreases, while the value of the Rotating parameter (Kr) increases, however, with decreasing in Viscosity parameter (R), f(η) extends in the range of [0, 1]. According to Fig. (3a), the velocity profile f'(η) for various value of the Magnetic parameter decreases when f'(η) is in the range of $\eta<\eta_m$. However, the velocity profile increases in the range of $\eta>\eta_m$. η_m is the location of the meeting of the curves for the different M at the same time. In addition, by reducing the amount of Viscosity parameter in Fig. (3a), the velocity profile decreases from the top plate to the lower plate. Fig. (3b) shows the influence of different Kr and δ parameters on f'(η). Based on this figure, the decreasing trend in f'(η) is observed when the amount of δ decreases. Besides, in this figure, with increasing the value of the Rotating parameter, the f'(η) profile in the range of $\eta<\eta_m$ has a drop, but f'(η) is increased inversely in the range of $\eta>\eta_m$. Fig. (4a) shows the impact of Viscosity and Melting parameters on g(η) velocity profile. According to this figure, with the decrease in δ and R parameters, the profile of g(η) decreases, while the value of this reduction for different values of δ is higher than R. The effect of the M and Kr parameters on g(η) is illustrated in Fig. (4b). According to this figure, it is seen that by decreasing the Magnetic parameter in the period of $\eta < \eta_m$, the velocity profile decreases, however, g(η) increases with an increase in Kr, although in the case of $\eta>\eta_m$, the process is entirely reversed. Changes of θ for various values of R and δ are shown in Fig. (5a). Based on this figure, while the Viscosity parameter increases, the temperature profile increases in the range of [0, 1], but with the increase in the Melting parameter, θ decreases. Fig. (5b) illustrates the effect of Nt and Nb parameters on the temperature profile. The temperature profile increases with increasing in Nt. Also, with a decrease in θ, the Brownian number also is decreased. Figs. 6 (a, b, c) show the effect of Sc, Nb, δ, Nt, R parameters on the concentration profile. As it is indicated in Figs. 6 (a) and (b), increasing the Viscosity parameter or decreasing the Brownian number decreases the concentration, while with the increase in the melting parameter or the decrease in the Thermophoretic parameter, ϕ has an ascending trend. Also, Fig. (6c) shows that the effect of Schmit parameter is very negligible on the concentration profile. The variations of the coefficient of surface friction in the period of [0.6] for various values of Nb, R, δ, Kr and Nt are given in Figs. 7 (a) and (b). According to these figures, with increasing in Rotating parameter or decreasing in Brownian number, the C_f profile increases from top to bottom plate. However, with decreasing in the Thermophoretic parameter or increasing in Melting parameter, C_f decreases, as well. It should be noted that, the Viscosity parameter does not have much influence on the surface friction coefficient profile. Figs. 8 (a) and (b) are plotted to show the effect of active parameters on the dimensionless Nusselt number. According to these figures, by increasing in Nt, R, and Nb, the Nu number has an ascending trend, while the dimensionless Nusselt number decreases by increasing in Melting parameter or Rotating parameter. It is mentionable that Kr changes affect slightly the Nu number. In addition, in order to better understanding the changes in velocity and concentration profiles which are mentioned in this research, contour plots of the effects of Viscosity and Melting parameters in the different range of η are demonstrated in Fig. (9). Additionally, in Fig. (10) convergence matter has been examined which reveals by increasing in the steps in our considered trial function we will get a correct solution.

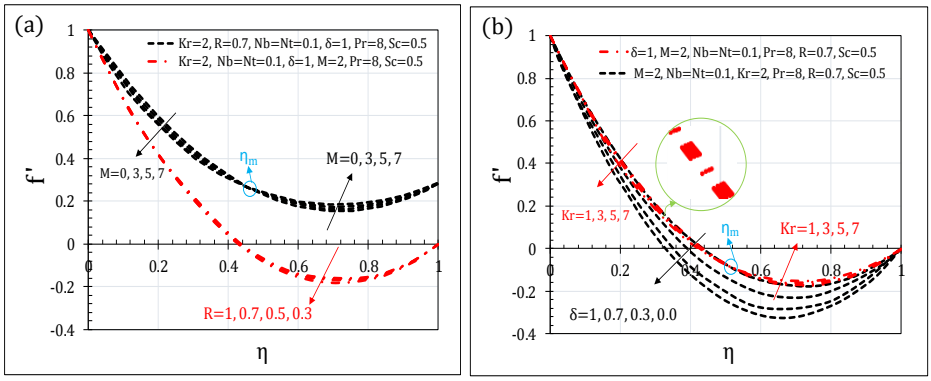

Figure 3. Influence of (a) M, R and (b) δ, Kr on velocity profiles.

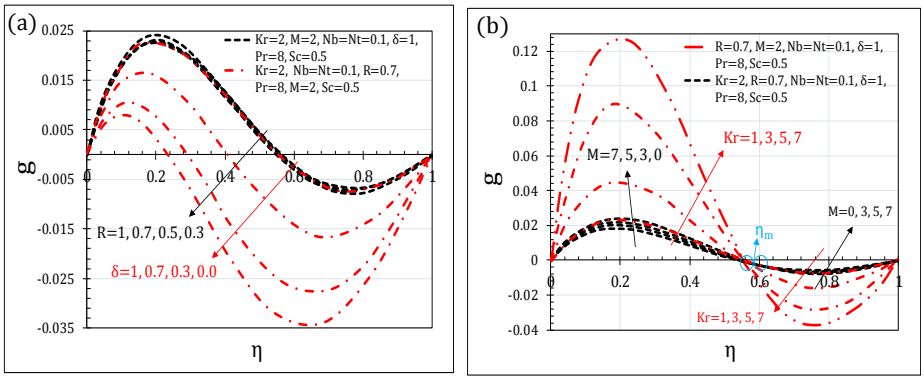

Figure 4. Influence of (a) δ, R and (b) M, Kr on velocity profiles.

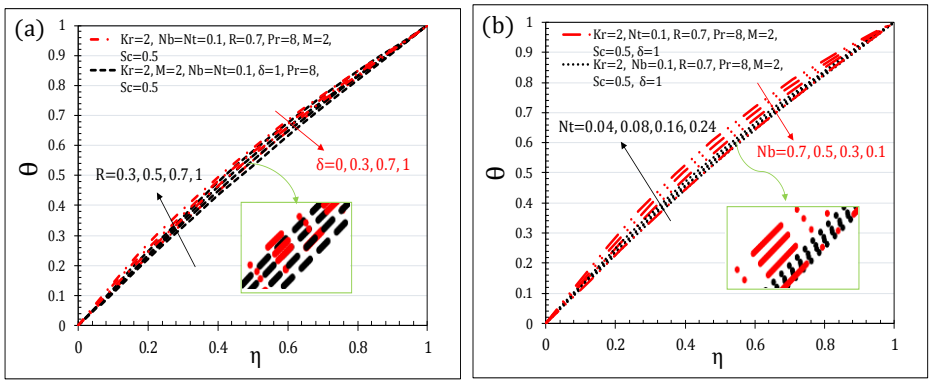

Figure 5. Influence of (a) δ, R and (b) Nt, Nb on temperature profiles.

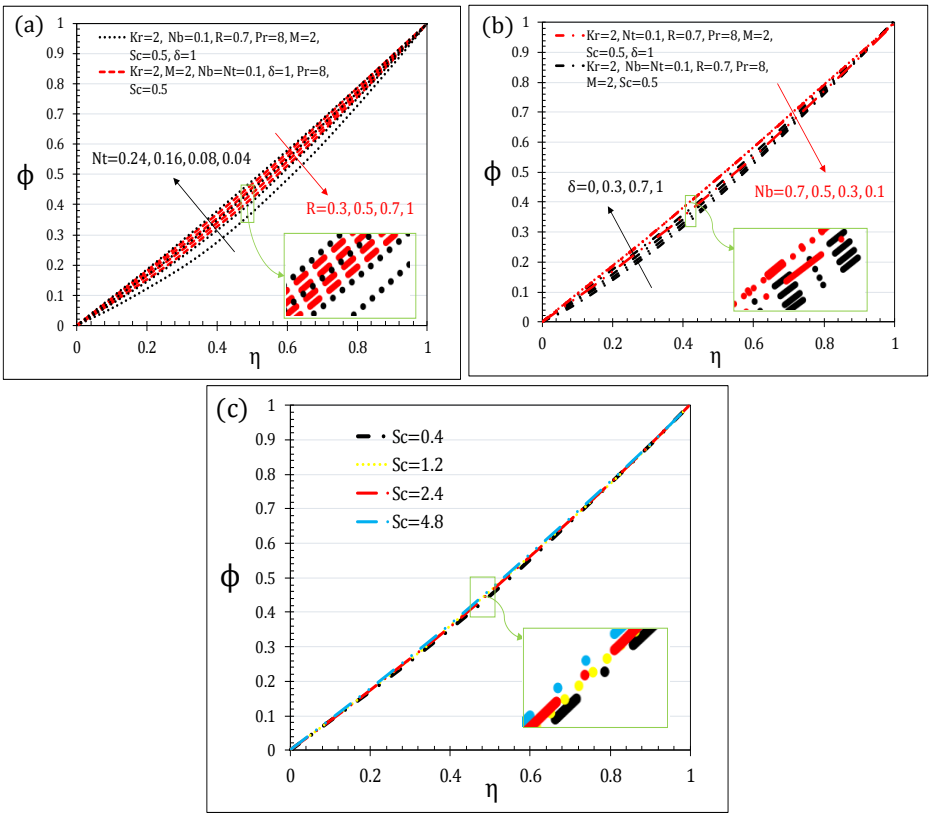

Figure 6. Influence of (a) Nt, R, (b) δ, Nb and (c) Sc on concentration profiles.

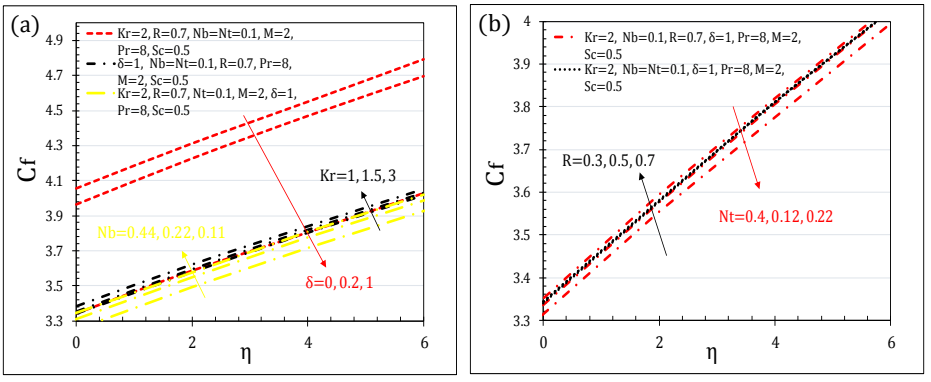

Figure 7. Influence of (a) Kr, Nb, δ and (b) R, Nt on skin friction coefficient.

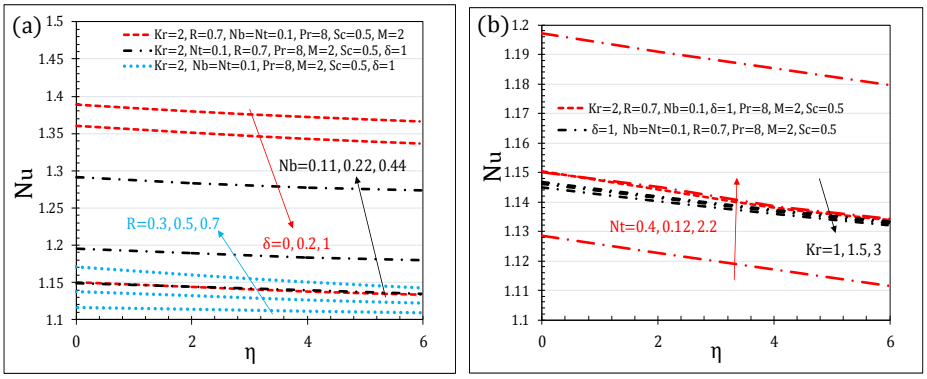

Figure 8. Influence of (a) R, Nb, δ and (b) Nt, Kr on Nusselt number.

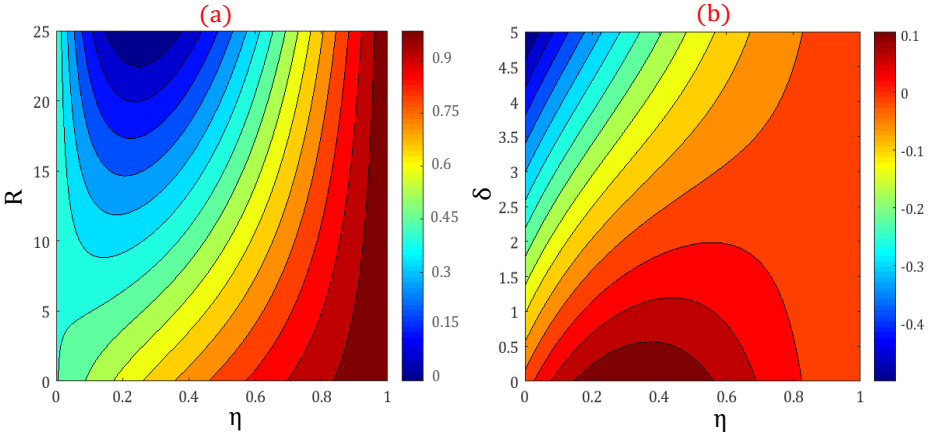

Figure 9. Contour plots of (a) Ø and (b) f, when Nt=Nb=0.1, Kr=1, M=1, Pr=10, Sc=1.

	Nomenclature		**Greek symbols**
B_0	Magnetic induction [tesla]	η	Similarity independent variable
D_B	Diffusion coefficient	ϕ	Volume fraction of nanofluid
			Dynamic viscosity
Ec	Eckert number	α	Thermal diffusivity [m^2/s]
Ha	Hartmann number	σ	Electrical conductivity
T_0	Initial temperature	δ	Melting parameter
T_m	Melting temperature		
Nt	Thermophoretic parameter		
Nb	Brownian motion parameter		
Sc	Schmidt number		
cs	Surface heat capacity		
T	Fluid temperature [K]		
Pr	Prandtl number		
v,u	Y and x directions velocity [m/s^2]		

Table 2. Comparison between the AGM and NUM [52] results for **θ (left)** and **ϕ (Right)**.

	Nt=Nb=0.1, M=Kr= δ=1, Pr=10			Nt=Nb=0.1, M=Kr= δ=1, Pr=10		
η	NUM	AGM	Error	NUM	AGM	Error
0.0	0.0000	0.0000	0.0000	0.0000	0.0000	0.0000
0.2	0.4415	0.2067	0.0016	0.1807	0.1998	0.0191
0.4	0.6261	0.4412	-0.0003	0.3685	0.3735	0.0068
0.6	0.8085	0.6253	-0.0008	0.5433	0.5424	-0.0009
0.8	1.0000	0.8076	-0.0009	0.7935	0.7919	-0.0016
1	1.0000	1.0000	0.0000	1.0000	1.0000	0.0000

6. CONCLUSIONS

In this research, we have tried to provide a solution to increase the heat transfer of Nanofluid flow in a two-phase revolving system with the presence of a magnetic field. For this purpose, a new method called AGM, a powerful method for solving nonlinear problems is introduced in this paper. Furthermore, the effect of various parameters such as Schmidt (Sc) number, Brownian (Nb) parameter, Magnetic parameter (M), Melting parameter (δ), Viscosity parameter (R), Rotating parameter (Kr) and Thermophoretic (Nt) parameter on the profiles of velocity (g(η), f'(η), f(η)), temperature profile (θ), concentration profile (ϕ), Nusselt number profile and surface friction coefficient (C_f) profile are investigated. Main outcomes are as follows:

- By increasing in Kr, the profile of f(η) decreases, while by decreasing in Viscosity parameter (R), f(η) increases in the range of [0, 1].
- By increasing in Viscosity parameter, the temperature profile increases in the range of [0, 1], but by increasing in Melting parameter, θ decreases.
- f'(η) increases in the range of $\eta>\eta_m$. Also, by increasing in Viscosity parameter or decreasing in Nb the concentration decreases, while by increasing in δ or decreasing in ϕ, Nt has an increasing trend.

It is worth mentioning that, Nanofluid heat transfer rate in a two-phase revolving system can be improved by controlling the magnetic field, and it will be evident that AGM is an excellent analytical method due to its efficiency for solving different problems.

REFERENCES

[1] Qayyum S, Khan R, Habib H. Simultaneous effects of melting heat transfer and inclined magnetic field flow of tangent hyperbolic fluid over a nonlinear stretching surface with homogeneous–heterogeneous reactions. International Journal of Mechanical Sciences. 2017 Nov 1; 133:1-0.

[2] Ibrahim W. Magneto hydrodynamic (MHD) boundary layer stagnation point flow and heat transfer of a nanofluid past a stretching sheet with melting. Propulsion and Power Research. 2017 Sep 1;6(3):214-22.

[3] Gupta S, Kumar D, Singh J. MHD mixed convective stagnation point flow and heat transfer of an incompressible nanofluid over an inclined stretching sheet with chemical reaction and radiation. International Journal of Heat and Mass Transfer. 2018 Mar 31; 118:378-87.

[4] Sheikholeslami, M., 2018. Application of Darcy law for nanofluid flow in a porous cavity under the impact of Lorentz forces. *Journal of Molecular Liquids*, *266*, pp.495-503.

[5] Sheikholeslami, M. and Rokni, H.B., 2018. CVFEM for effect of Lorentz forces on nanofluid flow in a porous complex shaped enclosure by means of non-equilibrium model. *Journal of Molecular Liquids*, *254*, pp.446-462.

[6] Sheikholeslami, M., Li, Z. and Shafee, A., 2018. Lorentz forces effect on NEPCM heat transfer during solidification in a porous energy storage system. *International Journal of Heat and Mass Transfer*, *127*, pp.665-674.

[7] Sheikholeslami, M., Shehzad, S.A., Abbasi, F.M. and Li, Z., 2018. Nanofluid flow and forced convection heat transfer due to Lorentz forces in a porous lid driven cubic enclosure with hot obstacle. *Computer Methods in Applied Mechanics and Engineering*, *338*, pp.491-505.

[8] Sheikholeslami, M. and Rokni, H.B., 2017. Numerical modeling of nanofluid natural convection in a semi annulus in existence of Lorentz force. *Computer Methods in Applied Mechanics and Engineering*, *317*, pp.419-430.

[9] Sheikholeslami, M., Shehzad, S.A. and Li, Z., 2018. Water based nanofluid free convection heat transfer in a three dimensional porous cavity with hot sphere obstacle in existence of Lorenz forces. *International Journal of Heat and Mass Transfer*, *125*, pp.375-386.

[10] Sheikholeslami, M., Mustafa, M.T. and Ganji, D.D., 2016. Effect of Lorentz forces on forced-convection nanofluid flow over a stretched surface. Particuology, 26, pp.108-113.

[11] Gireesha BJ, Mahanthesh B, Shivakumara IS, Eshwarappa KM. Melting heat transfer in boundary layer stagnation-point flow of nanofluid toward a stretching sheet with induced magnetic field. Engineering Science and Technology, an International Journal. 2016 Mar 31;19(1):313-21.

[12] Hsiao KL. Heat and mass mixed convection for MHD visco-elastic fluid past a stretching sheet with ohmic dissipation. Communications in Nonlinear Science and Numerical Simulation. 2010 Jul 31;15(7):1803-12.

[13] Zhang Y, Zhang M, Bai Y. Unsteady flow and heat transfer of power-law nanofluid thin film over a stretching sheet with variable magnetic field and power-law velocity slip effect. Journal of the Taiwan Institute of Chemical Engineers. 2017 Jan 31; 70:104-10.

[14] Sheikholeslami, M. and Ganji, D.D., 2017. Transportation of MHD nanofluid free convection in a porous semi annulus using numerical approach. Chemical Physics Letters, 669, pp.202-210.

[15] Dogonchi, A.S., Chamkha, A.J., Seyyedi, S.M. and Ganji, D.D., 2018. Radiative nanofluid flow and heat transfer between parallel disks with penetrable and stretchable walls considering Cattaneo–Christov heat flux model. *Heat Transfer—Asian Research*, *47*(5), pp.735-753.

[16] Alizadeh, M., Dogonchi, A.S. and Ganji, D.D., 2018. Micropolar nanofluid flow and heat transfer between penetrable walls in the presence of thermal radiation and magnetic field. *Case Studies in Thermal Engineering*, *12*, pp.319-332.

[17] Dogonchi, A.S. and Ganji, D.D., 2018. Effect of Cattaneo–Christov heat flux on buoyancy MHD nanofluid flow and heat transfer over a stretching sheet in the presence of Joule heating and thermal radiation impacts. *Indian Journal of Physics*, *92*(6), pp.757-766.

[18] Dogonchi, A.S. and Ganji, D.D., 2017. Analytical solution and heat transfer of two-phase nanofluid flow between non-parallel walls considering Joule heating effect. *Powder Technology*, *318*, pp.390-400.

[19] Dogonchi, A.S., Alizadeh, M. and Ganji, D.D., 2017. Investigation of MHD Go-water nanofluid flow and heat transfer in a porous channel in the presence of thermal radiation effect. *Advanced Powder Technology*, *28*(7), pp.1815-1825.

[20] Dogonchi, A.S. and Ganji, D.D., 2016. Thermal radiation effect on the Nano-fluid buoyancy flow and heat transfer over a stretching sheet considering Brownian motion. *Journal of Molecular Liquids*, *223*, pp.521-527.

[21] Dogonchi, A.S. and Ganji, D.D., 2016. Investigation of MHD nanofluid flow and heat transfer in a stretching/shrinking convergent/divergent channel considering thermal radiation. *Journal of Molecular Liquids*, *220*, pp.592-603.

[22] Dogonchi, A.S., Divsalar, K. and Ganji, D.D., 2016. Flow and heat transfer of MHD nanofluid between parallel plates in the presence of thermal radiation. *Computer Methods in Applied Mechanics and Engineering*, *310*, pp.58-76.

[23] Bai Y, Liu X, Zhang Y, Zhang M. Stagnation-point heat and mass transfer of MHD Maxwell nanofluids over a stretching surface in the presence of thermophoresis. Journal of Molecular Liquids. 2016 Dec 31; 224:1172-80.

[24] Khan WA, Khan M, Irfan M, Alshomrani AS. Impact of melting heat transfer and nonlinear radiative heat flux mechanisms for the generalized Burgers fluids. Results in Physics. 2017 Jan 1; 7:4025-32.

[25] Sheikholeslami, M. and Zeeshan, A., 2017. Analysis of flow and heat transfer in water based nanofluid due to magnetic field in a porous enclosure with constant heat flux using CVFEM. *Computer Methods in Applied Mechanics and Engineering*, *320*, pp.68-81.

[26] Sheikholeslami, M., 2018. CuO-water nanofluid flow due to magnetic field inside a porous media considering Brownian motion. *Journal of Molecular Liquids*, *249*, pp.921-929.

[27] Sheikholeslami, M., 2018. Influence of magnetic field on Al2O3-H2O nanofluid forced convection heat transfer in a porous lid driven cavity with hot sphere obstacle by means of LBM. *Journal of Molecular Liquids*.

[28] Dogonchi, A.S., Sheremet, M.A., Ganji, D.D. and Pop, I., 2018. Free convection of copper–water nanofluid in a porous gap between hot rectangular cylinder and cold circular cylinder under the effect of inclined magnetic field. *Journal of Thermal Analysis and Calorimetry*, pp.1-14.

[29] Sheikholeslami, M. and Rokni, H.B., 2018. Magnetic nanofluid flow and convective heat transfer in a porous cavity considering Brownian motion effects. *Physics of Fluids*, *30*(1), p.012003.

[30] Sheikholeslami, M., Shehzad, S.A., Li, Z. and Shafee, A., 2018. Numerical modeling for alumina nanofluid magnetohydrodynamic convective heat transfer in a permeable medium using Darcy law. *International Journal of Heat and Mass Transfer*, *127*, pp.614-622.

[31] Sheikholeslami, M., 2018. Solidification of NEPCM under the effect of magnetic field in a porous thermal energy storage enclosure using CuO nanoparticles. *Journal of Molecular Liquids*, *263*, pp.303-315.

[32] Mehrez Z, El Cafsi A, Belghith A, Le Quéré P. MHD effects on heat transfer and entropy generation of nanofluid flow in an open cavity. Journal of magnetism and Magnetic Materials. 2015 Jan 15; 374:214-24.

[33] Rana P, Dhanai R, Kumar L. MHD slip flow and heat transfer of Al 2 O 3-water nanofluid over a horizontal shrinking cylinder using Buongiorno's model: Effect of nanolayer and nanoparticle diameter. Advanced Powder Technology. 2017 Jul 31;28(7):1727-38.

[34] Mahanthesh B, Gireesha BJ, Gorla RS. Heat and mass transfer effects on the mixed convective flow of chemically reacting nanofluid past a moving/stationary vertical plate. Alexandria Engineering Journal. 2016 Mar 31;55(1):569-81.

[35] Mahanthesh B, Gireesha BJ, Gorla RS. Nonlinear radiative heat transfers in MHD three-dimensional flow of water based nanofluid over a non-linearly stretching sheet with convective boundary condition. Journal of the Nigerian Mathematical Society. 2016 Apr 30;35(1):178-98.

[36] Mahanthesh B, Gireesha BJ, Gorla RS. Unsteady three-dimensional MHD flow of a nano Eyring-Powell fluid past a convectively heated stretching sheet in the presence of thermal

radiation, viscous dissipation and Joule heating. Journal of the Association of Arab Universities for Basic and Applied Sciences. 2017 Jun 30; 23:75-84.

[37] Domairry, G. and Hatami, M., 2014. Squeezing Cu–water nanofluid flow analysis between parallel plates by DTM-Padé Method. *Journal of Molecular Liquids*, *193*, pp.37-44.

[38] Krishnamurthy MR, Prasannakumara BC, Gireesha BJ, Gorla RS. Effect of chemical reaction on MHD boundary layer flow and melting heat transfer of Williamson nanofluid in porous medium. Engineering Science and Technology, an International Journal. 2016 Mar 31;19(1):53-61.

[39] Bao SR, Zhang RP, Zhang YF, Tang Y, Zhang JH, Qiu LM. Enhancing the convective heat transfer in liquid oxygen using alternating magnetic fields. Applied Thermal Engineering. 2016 May 5; 100:125-32.

[40] Hayat T, Imtiaz M, Alsaedi A. Melting heat transfer in the MHD flow of Cu–water nanofluid with viscous dissipation and Joule heating. Advanced Powder Technology. 2016 Jul 31;27(4):1301-8.

[41] Sheikholeslami M, Rokni HB. Effect of melting heat transfer on nanofluid flow in the presence of a magnetic field using the Buongiorno Model. Chinese Journal of Physics. 2017 Jun 10.

[42] Sheikholeslami M, Rokni HB. Influence of melting surface on MHD nanofluid flow by means of two phase model. Chinese Journal of Physics. 2017 Aug 1;55(4):1352-60.

[43] Sheikholeslami M, Rokni HB. Melting heat transfer influence on nanofluid flow inside a cavity in existence of magnetic field. International Journal of Heat and Mass Transfer. 2017 Nov 1; 114:517-26.

[44] Dogonchi, A. S., and D. D. Ganji. "Investigation of heat transfer for cooling turbine disks with a non-Newtonian fluid flow using DRA." *Case Studies in Thermal Engineering* 6 (2015): 40-51.

[45] Ganji, D. D., and A. S. Dogonchi. "Analytical investigation of convective heat transfer of a longitudinal fin with temperature-dependent thermal conductivity, heat transfer coefficient and heat generation." *International Journal of Physical Sciences* 9, no. 21 (2014): 466-474.

[46] Dogonchi, A. S., M. Hatami, and G. Domairry. "Motion analysis of a spherical solid particle in plane Couette Newtonian fluid flow." *Powder Technology* 274 (2015): 186-192.

[47] Dogonchi, A. S., M. Hatami, Kh Hosseinzadeh, and G. Domairry. "Non-spherical particles sedimentation in an incompressible Newtonian medium by Padé approximation." *Powder Technology* 278 (2015): 248-256.

[48] Dogonchi, A. S., and D. D. Ganji. "Convection–radiation heat transfer study of moving fin with temperature-dependent thermal conductivity, heat transfer coefficient and heat generation." *Applied thermal engineering* 103 (2016): 705-712.

[49] Epstein M, Cho DH. Melting heat transfer in steady laminar flow over a flat plate. Journal of Heat Transfer. 1976 Aug 1;98(3):531-3.

[50] Vajravelu K, Kumar BV. Analytical and numerical solutions of a coupled non-linear system arising in a three-dimensional rotating flow. International Journal of Non-Linear Mechanics. 2004 Jan 31;39(1):13-24.

[51] Ahmadi A. Nonlinear Dynamic in Engineering by Akbari-Ganji's Method. Xlibris Corporation; 2015 Nov 10.

[52] Valipour P, Jafaryar M, Moradi R, Aski FS. Two phase model for nanofluid heat transfer intensification in a rotating system under the effect of magnetic field. Chemical Engineering and Processing: Process Intensification. 2018 Jan 31; 123:47-57.